Available online at www.sciencedirect.com

ScienceDirect

Mendeleev Commun., 2020, **30**, 728–730

Mendeleev Communications

New silver(I) thiazole-based coordination polymers: structural and photophysical investigation

Maxim I. Rogovoy,[a] Arina V. Tomilenko,[b] Denis G. Samsonenko,[a] Nina A. Nedolya,[c] Mariana I. Rakhmanova[a] and Alexander V. Artem'ev*[a]

[a] *A. V. Nikolaev Institute of Inorganic Chemistry, Siberian Branch of the Russian Academy of Sciences, 630090 Novosibirsk, Russian Federation. E-mail: chemisufarm@yandex.ru*

[b] *Department of Natural Sciences, Novosibirsk State University, 630090 Novosibirsk, Russian Federation*

[c] *A. E. Favorsky Irkutsk Institute of Chemistry, Siberian Branch of the Russian Academy of Sciences, 664033 Irkutsk, Russian Federation*

DOI: 10.1016/j.mencom.2020.11.013

Three 1D coordination polymers of $[Ag_2L_2(NO_3)_2]_n$ composition have been synthesized by the reaction of $AgNO_3$ with several disubstituted thiazoles. The building units of the polymers comprise two Ag atoms, which are μ_2-N,S-bridged by a pair of ligands in a head-to-tail manner. The UV-VIS solid-state dual emission has been found for the polymer with 4-methyl-2-(pyridin-3-yl)thiazole as a ligand.

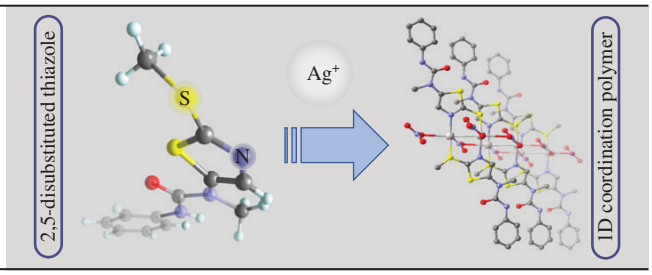

Keywords: silver(I) compound, coordination polymer, crystal structure, luminescence, dual emission.

Silver(I) complexes and coordination polymers (CPs) have gained attention due to their photoluminescence[1–3] and catalytic[4,5] properties as well as antimicrobial activity.[6,7] Ag^+ ion exhibits a variety of coordination geometries such as linear, tetrahedral, seesaw, square and octahedral ones.[8,9] Owing to this feature, Ag^I compounds demonstrate a great structural diversity.[10] As a result, their emissive properties can be fine-tuned varying the structural properties such as dimensionality and presence of site-specific interactions in the crystals.[11] The steric and electronic properties of a ligand environment primarily influence the emission type of the Ag^I complexes. Coordination compounds with O-, N- and S-donating ligands mostly exhibit intraligand fluorescence or phosphorescence[12,13] whereas complexes with P-donors reveal thermally activated delayed fluorescence.[14,15]

Among a plethora of ligands that are employed for design of Ag^I complexes, the thiazole ones are noteworthy due to their promising emissive properties and structural diversity of their Ag^I assemblies. Thus, anionic ligands of 2-mercaptobenzothiazole (Hmbt) assemble with silver(I) ions into hexanuclear $[Ag_6(mbt)_6]$ clusters[16–18] demonstrating near-infrared[17] and red luminescence.[18] Dithiazolylethene-based structures featuring photo-switchable fluorescence were also used for the synthesis of an Ag^I complex.[19] Coordination compounds with symmetric 1,3,5-tri- and hexa-thiazolylbenzene ligands were investigated as molecular flippers.[20] Meanwhile, despite a large number of available thiazole derivatives, there are a few examples of the corresponding luminescent Ag^I-based CPs.[21,22]

In this work, we report on the synthesis as well as structural and photophysical investigation of a series of structurally related 1D CPs derived from $AgNO_3$ and three disubstituted thiazole ligands **L1**–**L3**.

Our experiments have revealed that ligands **L1**–**L3** react with $AgNO_3$ in MeCN under ambient conditions within 1–10 min affording 1D CPs **1**–**3**, respectively, of $[Ag_2L_2(NO_3)_2]_n$ general formula in 70–75% yields (Figures 1–3).† Note that the reaction conditions such as reactant molar ratio from 2 : 1 to 1 : 2, solvent employed (CH_2Cl_2, EtOH, MeCN) and temperature do not actually affect the reaction outcome. Powder X-ray diffraction (PXRD) data of the as-synthesized samples reveal that the conditions used rule out the formation of side products for CPs **1** and **3**. On the contrary, the reaction of ligand **L2** with $AgNO_3$ suffers from a lack of selectivity, so the phase-pure powder of CP **2** has not been obtained. The CPs synthesized exhibit 1D structural motifs that depend on the ligand used. Ligands within the CPs designed differ in the coordination pattern demonstrating either N,N- (for ligands **L1** and **L2**) or 1,3-N,S one for ligand **L3**. Consequently, CPs **1** and **2** contain chain-like motif, whereas CP **3** has a stacked structure

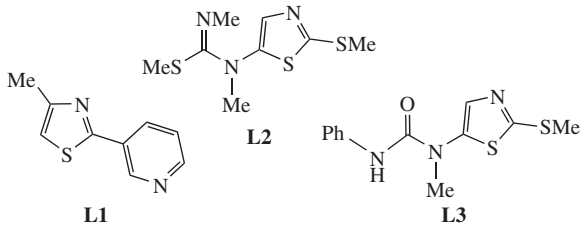

† Single crystals of compounds **1**–**3** were grown by a slow diffusion of diethyl ether vapors into their acetonitrile solutions. Diffraction data were obtained using an automated Agilent Xcalibur diffractometer equipped with an AtlasS2 area detector (MoKα, graphite monochromator, ω-scans) at 140 K. Integration, absorption correction and determination of unit cell parameters were performed using CrysAlis^{Pro} version 1.171.38.46. The structures were solved by dual space algorithm (SHELXT)[23] and refined by the full-matrix least squares technique (SHELXL)[24] in the anisotropic approximation, except for hydrogen atoms. Positions of hydrogen atoms of organic ligands were calculated geometrically and refined according to the riding model.

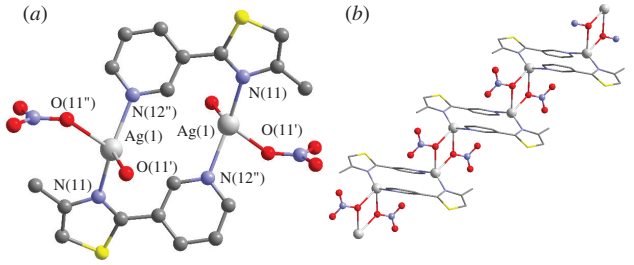

Figure 1 (*a*) $[Ag_2L_2(NO_3)_2]$ as the building unit of CP **1** and (*b*) the polymeric structure of CP **1**. Selected bond lengths (Å) and angles (°): Ag(1)–O(11)' 2.4828(16), Ag(1)–N(11) 2.2149(17), Ag(1)–O(11') 2.5661(17), Ag(1)–N(12") 2.2353(19), O(11)–Ag(1)–O(11') 74.45(6), N(12")–Ag(1)–O(11') 82.94(6), N(11)–Ag(1)–O(11) 103.32(6), N(12")–Ag(1)–O(11) 108.83(6), N(11)–Ag(1)–O(11)' 122.81(6), Ag(1)–O(11)–Ag(1)' 105.55(6), N(11)–Ag(1)–N(12)" 143.51(6). Symmetry codes: (') 2–*x*, 2–*y*, 2–*z*; (") 1–*x*, 2–*y*, 2–*z*.

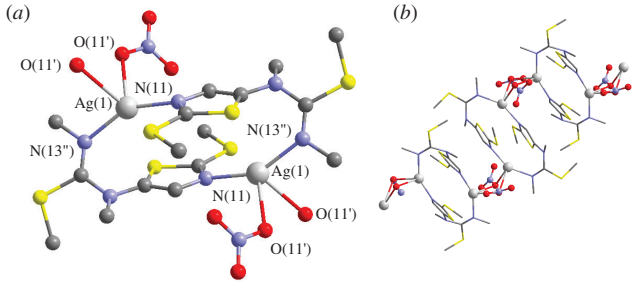

Figure 2 (*a*) $[Ag_2L_2(NO_3)_2]$ as the building unit of CP **2** and (*b*) the polymeric structure of CP **2**. Selected bond lengths (Å) and angles (°): Ag(1)–O(11') 2.4553(12), Ag(1)–N(11) 2.1967(13), Ag(1)–O(11') 2.5976(12), Ag(1)–N(13") 2.2329(14), O(11)–Ag(1)–O(11') 69.23(5), N(13")–Ag(1)–O(11') 88.93(4), N(11)–Ag(1)–O(11') 105.07(5), N(13")–Ag(1)–O(11') 102.21(5), N(11)–Ag(1)–O(11') 112.08(5), N(11)–Ag(1)–N(13") 150.07(5). Symmetry codes: (') 1–*x*, *y*, 3/2–*z*; (") 1–*x*, 1–*y*, 1–*z*.

(*vide infra*). The compounds obtained represent crystalline powders well soluble in MeCN and EtOH. According to thermogravimetric analysis (TGA), CPs **1** and **3** are stable up to 150 and 200 °C, respectively. Both their TG curves display a complex multistep decomposition pattern (Figure S4, see Online Supplementary Materials). Henceforth, CPs **1** and **3** were characterized using single crystal X-ray diffractometry (sc-XRD), elemental analysis, thermogravimetry and FT-IR spectroscopy, while CP **2** was explored by sc-XRD only.

The FT-IR spectra of complexes **1** and **3** contain strong bands at 1380–1550 cm^{-1}, which indicate the presence of N–O stretching vibrations of the NO_3 moieties. Also, a weak band at 1760 (or 1730) cm^{-1} for CP **1** (or CP **3**) is attributed to the ligand, namely, C=N stretching vibrations of the thiazole ring (Figure S5, see Online Supplementary Materials).

Although compounds **1** and **2** belong to different, namely triclinic $P\bar{1}$ and orthorhombic *Pbcn* space groups, respectively, they have similar structural features. Their building units comprise two Ag atoms, a pair of ligands and two NO_3^- ions. The ligands **L1** and **L2** both adopt μ_2-N,N bridging mode and thus coordinate to two metal centers in a head-to-tail fashion [see Figures 1(*a*), 2(*a*)]. NO_3^- ion completes the coordination environment of each silver atom into a $\{Ag@N_2O_2\}$ geometry, which can be described as intermediate between the tetrahedral and seesaw ones (the four-coordinate geometry indices are $\tau_4 = 0.66$, $\tau_4' = 0.73$ for CP **1** and $\tau_4 = 0.69$, $\tau_4' = 0.81$ for CP **2**).[25] NO_3^- ions serve also as linkers between the building units to form 1D coordination chains [see Figure 1(*b*)]. As displayed in Figures 1(*b*) and 2(*b*), the units are connected *via* four-membered $\{Ag_2(NO_3)_2\}$ cycles with the Ag···Ag distances being as large as 4.0208(4) and 5.0056(4) Å for CPs **1** and **2**, respectively, which is too long for any argentophilic interactions. However, there are some weak van der Waals interactions (C_{Ar}···C_{Ar}, S···ONO_3, Ag···N, *etc.*), which enable the interconnection of the 1D chains [Figure S1(*a*),(*b*), see Online Supplementary Materials].

CP **3** crystallizes in monoclinic $P2_1/c$ space group and its building unit contains a pair of Ag atoms, two ligands **L3** and two NO_3^- ions [see Figure 3(*a*)]. In contrast to **L1** and **L2**, ligand **L3** exhibits N,S-bridging coordination mode. A relatively close disposition of the N and S donor atoms favours formation of the $[Ag(^{SCN}_{NCS})Ag]$ metallacycle. Two NO_3^- ions complete the silver coordination sphere making each metal center four-coordinated, the $\{Ag@O_2NS\}$ geometry being close to tetrahedral one ($\tau_4 = 0.69$, $\tau_4' = 0.76$). Moreover, nitrate groups with a bidentate μ_2-O,O mode are responsible for the formation of chain-like 1D polymer

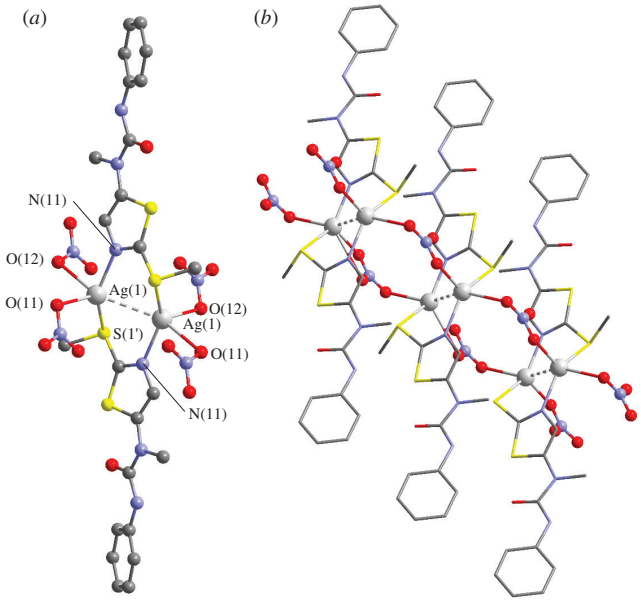

Figure 3 (*a*) $[Ag_2L_2(NO_3)_2]$ as the building unit of CP **3** and (*b*) the polymeric structure of CP **3**. Selected bond lengths (Å) and angles (°): Ag(1)–N(11) 2.2295(15), Ag(1)–S(1') 2.4829(5), Ag(1)–O(11) 2.4579(14), Ag(1)–O(12) 2.6075(14), N(11)–Ag(1)–O(11) 97.85(5), N(11)–Ag(1)–O(12) 88.95(5), N(11)–Ag(1)–S(1') 141.92(4), O(11)–Ag(1)–O(12) 94.65(4), O(11)–Ag(1)–S(1') 120.15(3), S(1')–Ag(1)–O(12) 90.30(3). Symmetry codes: (') 2–*x*, 1–*y*, 2–*z*; (") *x*–1, *y*, *z*.

Crystal data for **1**. $C_9H_8AgN_3O_3S$, M = 346.11, triclinic, space group $P\bar{1}$, T = 140 K, a = 8.0721(5), b = 9.0383(5) and c = 9.3768(4) Å, α = = 115.578(5), β = 96.058(4) and γ = 110.661(5)°, V = 549.77(6) Å^3, Z = 2, d_{calc} = 2.091 g cm^{-3}, μ(MoKα) = 0.71073 cm^{-1}. 8560 reflections were measured and 2574 independent reflections (R_{int} = 0.025) were used for further refinement. The refinement converged to wR_2 = 0.046 and GOF = = 1.062 for all independent reflections [R_1 = 0.022 was calculated against F for the 2324 observed reflections with $I > 2\sigma(I)$].

Crystal data for **2**. $C_8H_{13}AgN_4O_3S_3$, M = 417.27, orthorhombic, space group *Pbcn*, T = 140 K, a = 18.8742(5), b = 11.3371(3) and c = 13.6760(3) Å, V = 2926.37(13) Å^3, Z = 8, d_{calc} = 1.894 g cm^{-3}, μ(MoKα) = 0.71073 cm^{-1}. 13507 reflections were measured and 3621 independent reflections (R_{int} = 0.018) were used for further refinement. The refinement converged to wR_2 = 0.047 and GOF = 1.05 for all independent reflections [R_1 = 0.020 was calculated against F for the 3206 observed reflections with $I > 2\sigma(I)$].

Crystal data for **3**. $C_{12}H_{13}AgN_4O_4S_2$, M = 449.25, monoclinic, space group $P2_1/c$, T = 140 K, a = 5.75973(17), b = 27.3118(9) and c = 9.9641(3) Å, β = 97.135(3)°, V = 1555.30(8) Å^3, Z = 4, d_{calc} = 1.919 g cm^{-3}, μ(MoKα) = = 0.71073 cm^{-1}. 26097 reflections were measured and 4015 independent reflections (R_{int} = 0.027) were used for further refinement. The refinement converged to wR_2 = 0.050 and GOF = 1.07 for all independent reflections [R_1 = 0.023 was calculated against F for the 3565 observed reflections with $I > 2\sigma(I)$].

CCDC 1994453–1994455 contain the supplementary crystallographic data for this paper. These data can be obtained free of charge from The Cambridge Crystallographic Data Centre *via* http://www.ccdc.cam.ac.uk.

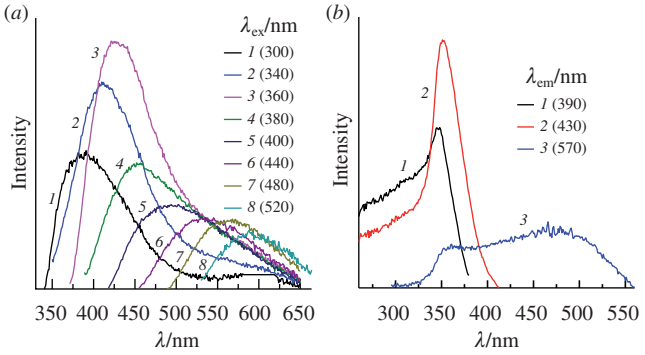

Figure 4 (*a*) Emission and (*b*) excitation spectra of CP **1** at T = 300 K.

[see Figure 3(*b*)]. Both Ag atoms are arranged to provide argentophilic interactions of 3.0086(5) Å (*cf.* sum of the Ag van der Waals radii equal to 3.44 Å). In the crystal of CP **3**, the 1D chains are stitched by weak van der Waals interactions [C_{Ar}–H···O–N, C_{Me}–H···C and C_{Me}···C_{Me}, Figure S1(*c*), see Online Supplementary Materials].

CPs **2** and **3** have no apparent luminescence under ambient conditions and virtually no emission upon cooling to 77 K. On the contrary, CP **1** demonstrates luminescence in both UV and visible ranges (300–520 nm). The emission spectrum of CP **1** features two broad bands at 380 and 570 nm [Figure 4(*a*)]. Also, the emission maxima and intensities of the bands vary with the excitation wavelength. Thus, shorter excitation wavelengths of 300–380 nm give rise to a high energy (HE) band, whereas larger λ_{ex} values (380–520 nm) contribute to a low energy (LE) band [Figure 4(*b*)]. To explain the origin of the two bands, their emission lifetimes τ were measured for both HE and LE bands. The τ values of 1.7 ns and 3.5 ms clearly point to fluorescence and phosphorescence mechanisms, respectively. According to the known data on silver complexes with 2-thiazolyl sulfides[26] and various Ag^I-containing polyoxometallates,[27–29] the two bands are likely originated from intraligand Ag^I-perturbed fluorescence and phosphorescence.

In summary, the direct reaction between $AgNO_3$ and three thiazole ligands affords one-dimensional Ag^I coordination polymers featuring the same composition $[Ag_2L_2(NO_3)_2]_n$. A detailed photophysical study has demonstrated that the CP derived from 4-methyl-2-(pyridin-3-yl)thiazole exhibits a dual emission wavelength-dependent luminescence. Overall, these findings contribute to the design of new luminescent silver(I) thiazole coordination polymers.

This work was supported by the Russian Science Foundation (grant no. 18-73-10086).

Online Supplementary Materials

Supplementary data associated with this article can be found in the online version at doi: 10.1016/j.mencom.2020.11.013.

References

1 Y.-C. He, N. Xu, X. Zheng, Y. Yu, B. Ling and J. You, *Dyes Pigm.*, 2017, **136**, 577.
2 J. Yan, L. Wilbraham, P. N. Basa, M. Schüttel, J. C. MacDonald, I. Ciofini, F.-X. Coudert and S. C. Burdette, *Inorg. Chem.*, 2018, **57**, 15009.
3 Y.-L. Wang, Q.-Y. Liu and L. Xu, *CrystEngComm*, 2008, **10**, 1667.
4 A. Liu, C.-C. Wang, C.-z. Wang, H.-f. Fu, W. Peng, Y.-L. Cao, H.-Y. Chu and A.-F. Du, *J. Colloid Interface Sci.*, 2018, **512**, 730.
5 C.-c. Wang, H.-p. Jing and P. Wang, *J. Mol. Struct.*, 2014, **1074**, 92.
6 S. Medici, M. Peana, G. Crisponi, V. M. Nurchi, J. I. Lachowicz, M. Remelli and M. A. Zoroddu, *Coord. Chem. Rev.*, 2016, **327–328**, 349.
7 S. H. Alisir, S. Demir, B. Sariboga and O. Buyukgungor, *J. Coord. Chem.*, 2015, **68**, 155.
8 F. A. Cotton and G. Wilkinson, *Advanced Inorganic Chemistry*, 5th edn., John Wiley & Sons, Inc., 1988.
9 M. I. Rogovoy, M. P. Davydova, I. Yu. Bagryanskaya and A. V. Artem'ev, *Mendeleev Commun.*, 2020, **30**, 305.
10 H.-Q. Huang, X.-Y. Cheng, T. Zhang and R.-B. Huang, *Inorg. Chem. Commun.*, 2016, **68**, 21.
11 S.-Z. Zhan, H.-Q. Song, L.-J. Guo, R. W.-Y. Sun and D. Li, *Eur. J. Inorg. Chem.*, 2017, 5127.
12 S. Igawa, M. Hashimoto, I. Kawata, M. Hoshino and M. Osawa, *Inorg. Chem.*, 2012, **51**, 5805.
13 C.-W. Hsu, C.-C. Lin, M.-W. Chung, Y. Chi, G.-H. Lee, P.-T. Chou, C.-H. Chang and P.-Y. Chen, *J. Am. Chem. Soc.*, 2011, **133**, 12085.
14 H. Yersin, R. Czerwieniec, M. Z. Shafikov and A. F. Suleymanova, *ChemPhysChem*, 2017, **18**, 3508.
15 M. Z. Shafikov, A. F. Suleymanova, A. Schinabeck and H. Yersin, *J. Phys. Chem. Lett.*, 2018, **9**, 702.
16 S. Lin, Y.-Z. Cui, Q.-M. Qiu, H.-L. Han, Z.-F. Li, M. Liu, X.-L. Xin and Q.-H. Jin, *Polyhedron*, 2017, **134**, 319.
17 C. Yue, C. Yan, R. Feng, M. Wu, L. Chen, F. Jiang and M. Hong, *Inorg. Chem.*, 2009, **48**, 2873.
18 S.-C. Chen, R.-M. Yu, Z.-G. Zhao, S.-M. Chen, Q.-S. Zhang, X.-Y. Wu, F. Wang and C.-Z. Lu, *Cryst. Growth Des.*, 2010, **10**, 1155.
19 M. Giraud, A. Léaustic, R. Guillot, P. Yu, P. G. Lacroix, K. Nakatani, R. Pansu and F. Maurel, *J. Mater. Chem.*, 2007, **17**, 4414.
20 S. Hiraoka, K. Harano, T. Tanaka, M. Shiro and M. Shionoya, *Angew. Chem., Int. Ed.*, 2003, **42**, 5182.
21 S. J. Bullock, F. S. Davidson, R. A. Faulkner, G. M. B. Parkes, C. R. Rice and L. Towns-Andrews, *CrystEngComm*, 2017, **19**, 1273.
22 N. Rahanyan, S. Duttwyler, A. Linden, K. K. Baldridge and J. S. Siegel, *Dalton Trans.*, 2014, **43**, 11027.
23 G. M. Sheldrick, *Acta Crystallogr., Sect. A: Found. Adv.*, 2015, **71**, 3.
24 G. M. Sheldrick, *Acta Crystallogr., Sect C.: Struct. Chem.*, 2015, **71**, 3.
25 L. Yang, D. R. Powell and R. P. Houser, *Dalton Trans.*, 2007, 955.
26 M. I. Rogovoy, D. G. Samsonenko, M. I. Rakhmanova and A. V. Artem'ev, *Inorg. Chim. Acta*, 2019, **489**, 19.
27 A. V. Chupina, V. Shayapov, A. S. Novikov, V. V. Volchek, E. Benassi, P. A. Abramov and M. N. Sokolov, *Dalton Trans.*, 2020, **49**, 1522.
28 A. V. Chupina, A. A. Mukhacheva, P. A. Abramov and M. N. Sokolov, *J. Struct. Chem.*, 2020, **61**, 299 (*Zh. Strukt. Khim.*, 2020, **61**, 315).
29 A. A. Shmakova, A. S. Berezin, P. A. Abramov and M. N. Sokolov, *Inorg. Chem.*, 2020, **59**, 1853.

Received: 13th June 2020; Com. 20/6237